

Synthesis of oleic-imidazoline and investigation on its inhibition efficiency for the corrosion of low carbon steel in chloride environments

D.U.C Rahayu,^{1*} Y.K. Krisnandi,¹ B.H. Susanto,² I. Abdullah,¹
D.A. Nurani,¹ I.R. Saragi,^{1,3} A. Yuniastuti,¹ M. Mujahiduzzakka,¹
S. Cahyani,¹ S. Fitriani,¹ F.G. Nurchanifah,¹ R.A. Fadhilsyah,¹
B. Purnomo⁴ and A.P. Gustianthy⁴

¹Department of Chemistry, Faculty of Mathematics and Natural Sciences (FMIPA),
Universitas Indonesia, Depok 16424, Indonesia

²Department of Chemical Engineering, Faculty of Engineering, Universitas Indonesia,
Depok 16424, Indonesia

³Department of Chemistry, Faculty of Mathematics and Natural Sciences (FMIPA),
Universitas Sumatera Utara, Medan 20155, Indonesia

⁴PT Pertamina Research and Technology Center, Jl. Raya Bekasi Km.20, Pulogadung,
Jakarta 13920, Indonesia

*E-mail: dyahutamir@sci.ui.ac.id

Abstract

Carbon steel is the principal material used in oil and gas production pipelines. However, carbon steel is vulnerable to corrosion by corrosive media it contacts, and this causes economic losses. The corrosion rate of carbon steel is inhibited by imidazoline, an organic corrosion inhibitor. In this study, oleic-imidazoline was successfully synthesized from triethylenetetramine and oleic acid under reflux at 100–140°C for 12 h. The synthesized compound was characterized for its structure by using FTIR, UV-Vis, NMR (¹H and ¹³C), and LC-MS/MS spectral data. Oleic-imidazoline showed a maximum absorption peak at a wavelength of 203.8 nm (UV-Vis), absorption peaks at 1656.51 cm⁻¹ belonging to C=N bond (FTIR), a peak at a chemical shift of 2.17 and 3.30–3.48 ppm indicating $\underline{\text{H}}-\text{C}-\text{C}=\text{N}$ and imidazoline ring proton, respectively (¹H NMR), and a peak at the chemical shift of 164.6 ppm fitting C=N (¹³C NMR). LC-MS/MS showed that oleic-imidazoline was a major component in the synthesized compound with $[\text{M}+\text{H}]^+$ 393.37 *m/z* at *rt* 10.87 min. The oleic-imidazoline's performance as a corrosion inhibitor toward low carbon steel in a 1% NaCl solution was measured using two methods, which are Tafel polarization and weight loss. The highest inhibition efficiency percentage (%*IE*) resulted from the two methods are 83.26% and 83.33%, respectively. Oleic-imidazoline reveals good performance to inhibit the corrosion since this compound undergoes physisorption with slight chemisorption on low carbon steel in chloride environment.

Received: July 16, 2021. Published: September 10, 2021

doi: [10.17675/2305-6894-2021-10-3-25](https://doi.org/10.17675/2305-6894-2021-10-3-25)

Keywords: chloride environment, corrosion inhibitor, low carbon steel, oleic-imidazoline.

1. Introduction

Carbon steel is the most commonly used material in oil and gas pipelines for production lines. Because of its corrosive medium, however, carbon steel is susceptible to corrosion, resulting in financial losses [1]. Therefore, one of the organic corrosion inhibitors, imidazoline, has been used to slow the corrosion rate of carbon steel [2]. Imidazoline is a heterocyclic compound containing high electron density centres, which leads to the protection of metal surfaces from corrosion [3]. The addition of heterocyclic compound as a corrosion inhibitor has recently become more popular since the use of this compound leads to a more biodegradable, inexpensive, and environmentally friendly corrosion control technique [4]. A corrosion inhibitor based on the imidazoline scaffold affects anodic and cathodic reactions with the adsorption process on metal surfaces [5]. Furthermore, imidazoline has a good adsorption character and can form a protective layer (film) on metal surfaces and a monolayer that has hydrophobic properties [6–8].

Research on the structural modification of imidazoline (especially oleic-imidazoline) as a corrosion inhibitor has been carried out. Zhao *et al.*, (2016) had synthesized oleic-imidazoline from oleic acid (OA) and various polyamines such as ethylenediamine (EDA), diethylenetriamine (DETA), triethylenetetramine (TETA), tetraethylenepentamine (TEPA), polyethylenepolyamine (PEPA) and aminoethylethanolamine (AEEA). The hydroxyethyl group in the pendant chain can increase the hydrophilicity, whereas the aminoethyl group will increase the hydrophobicity. Oleic-imidazoline which showed the highest activity as a corrosion inhibitor on the oil field in China was from DETA and TETA [9]. Modification of oleic-imidazoline from DETA had been intensively carried out to form quaternary oleic-imidazoline which showed a 99.113% corrosion inhibition rate in hydrochloric acid [10]. Furthermore, oleic-imidazoline from TEPA and ester form of oleic-imidazoline from AEEA showed a good performance as a corrosion inhibitor in 1% NaCl [11, 12]. In addition, oleic-imidazoline from DETA, AEEA and TETA exhibited high activity to inhibit the corrosion in sulfuric acid with the addition of inorganic salts, *i.e.* KI, KCNS and KCl [13]. All the aforementioned research above revealed that oleic-imidazoline had a good potential to inhibit corrosion. Therefore, in this study, synthesis of oleic-imidazoline from TETA and technical grade of OA was conducted followed by investigating its anticorrosion activity in chloride environment. TETA was chosen as polyamines since oleic-imidazoline synthesized from TETA for both structural elucidation and its corrosion inhibition activity is still limited. Meanwhile, the technical grade of OA was selected since it was economically friendly, which has the potential to be used in the industrial scale. Synthesizing and developing oleic-imidazoline could provide an alternative for organic corrosion inhibitor uses for both research and industrial applications.

2. Experimental

2.1. General

The chemicals used for synthesis, test, and analysis were triethylenetetramine (TETA), NaCl, CH₂Cl₂, acetone, methanol (MeOH), NH₄OH 25%, and Na₂SO₄ anhydrous purchased from Merck, while the technical grade of oleic acid (OA) from PT. Brataco Chemika with a composition of 80.80% OA, <18% linoleic acid (LNA), and <6% stearic acid (SA). All chemicals were used without any purification before use. Oleic-imidazoline was synthesized by reflux method which required a three-neck round-bottom flask, condenser, oil bath, magnetic stirrer, hot plate, and thermometer. The reaction was monitored using thin-layer chromatography (TLC) on precoated 0.25 mm thickness of Si 60 GF₂₅₄ plates (Merck) and TLC spots were visualized under UV₂₅₄. The corrosion inhibition activity tests were performed using an electrochemical method with an eDAQ 450 potentiostat-Versasat II and gravimetric method. The materials used for corrosion inhibition activity tests were a low carbon steel JIS G3123 grade SGD 400D with a diameter of 5 mm and a length of 4–5 cm obtained from PT. Citra Tanamas with a composition of C 0.08%, 0.40% Mn, 0.19% Si, 0.033% P, 0.021% S, and 99.276% Fe as working electrode (WE), SCE as reference electrode (RE), and platinum as auxiliary electrode (AE). As a comparison, the commercial sample of corrosion inhibitor was obtained from PT. Pertamina (Persero). UV-Vis Shimadzu UV2540 in MeOH spectroscopic grade (Merck), FTIR Shimadzu IR Prestige 2 in KBr pellet (Merck), 500 MHz NMR Bruker Avance operating at 500 MHz (¹H) and 125 MHz (¹³C) in CDCl₃ (Merck), and LC-MS/MS with LC system ACQUITY UPLC® H-Class System (Waters, USA) and MS Xevo G2-S QToF (Waters, USA) in MeOH spectroscopic grade (Merck) with the addition of formic acid (Merck) were used for structural elucidation of oleic-imidazoline. LC-MS/MS parameters were adapted from previous research [14].

2.2. Synthesis of oleic-imidazoline

Oleic-imidazoline was synthesized from TETA (5 mmol) and OA (5 mmol) in a three-neck round-bottom flask connected to a condenser equipped with a magnetic stirrer and thermometer. After heating with reflux at 100–140°C for 12 hours, the mixture then was worked up by extraction by using CH₂Cl₂: brine solution (1:1, v/v) to collect the organic layer. The organic layer then was dried using Na₂SO₄ anhydrous, evaporated, and stored in a desiccator. The synthesized compound then was identified using TLC with CH₂Cl₂: MeOH (8:2, v/v) with one drop of NH₄OH 25% as an eluent, and further characterized by using FTIR, UV-Vis, NMR (¹H and ¹³C), and LC-MS/MS.

Oleic-imidazoline was obtained as dark-brown oily-solid, *R*_f 0.80 in CH₂Cl₂: MeOH (8:2, v/v) with one drop of NH₄OH 25%; FTIR (KBr pellet) ν_{\max} (cm⁻¹): 3291.83 (N–H), 3008.25 (C–H sp²), 2924.75–2853.07 (C–H sp³), 1656.51 (C=N), 1643.12 (C=C), 1547.80 (N–H), 1465.09–1375.29 (C–H sp³), 1271.31 (=C–N), 723.84 (*cis* C–H); UV-Vis (MeOH) λ_{\max} (nm): 203.8; ¹H NMR (500 MHz, CDCl₃) δ (ppm): 5.33 (2H, *q*, 7 Hz), 4.23 (3H, *br s*),

3.62–3.26 (4H, *m*), 2.92–2.42 (8H, *m*), 2.16 (2H, *t*, 7 Hz), 2.01 (4H, *q*, 7 Hz), 1.59 (2H, *qi*, 9.5 Hz), 1.37–1.24 (20H, *m*), 0.87 (3H, *t*, 7 Hz); ^{13}C NMR (125 MHz, CDCl_3) δ (ppm): 164.6, 130.1, 129.9, 56.7, 54.3, 54.1, 53.2, 52.9, 52.9, 32.0, 29.9, 29.8 (4C), 29.7, 29.5, 29.4, 29.3 (2C), 27.3, 25.7, 22.8, 14.3; and LC-MS/MS (MeOH–HCOOH): dominant LC rt 10.87 min, MS (25–60 eV, *m/z*): 393.37 $[\text{M}+\text{H}]^+$ calculated as $\text{C}_{24}\text{H}_{49}\text{N}_4^+$, 376.34, 349.33, 320.30, 308.30, 306.28 (base peak), 280.26, 268.27, 254.25, 238.22, 224.20, 210.19, 196.17, 184.16, 170.13, 156.13, 141.10, 127.09, 113.07, 98.06, 87.09, 71.06.

2.3. Tafel polarization method

Electrochemical measurements were conducted using the cyclic voltammetry method in a 1% NaCl saturated with CO_2 based on previous work [11]. Three electrodes, WE, RE, and AE, were arranged as an electrochemical cell in a beaker glass which contained corrosion medium solution in the absence and presence of various concentrations of corrosion inhibitor (100–500 ppm). The potentiodynamic polarization then was recorded within the potential range of -2000 to $+500$ mV at a potential scan rate of 50 mV/s. The electrochemical parameters and the percentage of inhibition efficiency (%*IE*) were obtained by using the Tafel polarization which was processed by using Equation 1 while the corrosion rate (C_R in $\text{mm}\cdot\text{y}^{-1}$) was evaluated using Equation 2, where I_{corr}^0 and I_{corr} (mA/cm^2) is corrosion current densities in the absence and presence of corrosion inhibitor, respectively, *K* represents rate constant, *EW* represents equivalent weight in g/equiv., *d* represents tested low carbon steel density (g/cm^3), whereas *A* is the area of the sample (cm^2).

$$\%IE = \left(1 - \frac{I_{\text{corr}}}{I_{\text{corr}}^0}\right) \cdot 100 \quad (1)$$

$$C_R = \frac{I_{\text{corr}} \cdot K \cdot EW}{d \cdot A} \quad (2)$$

2.4. Weight loss method

Gravimetric measurements were carried out in a 1% NaCl environment in the presence of various concentrations of corrosion inhibitor (100–500 ppm). The soaking time was adjusted for 6 h at room temperature. After soaking, low carbon steel was removed from the corrosion medium solution and washed with bi-distilled water and acetone, then dried and weighed. The results obtained then were compared with low carbon steel immersed in the corrosion medium without the addition of oleic-imidazoline. The C_R ($\text{mm}\cdot\text{y}^{-1}$) and %*IE* were calculated following Equations 3 and 4, respectively, where *W* represents weight loss (mg), *d* represents tested low carbon steel density (g/cm^3), *A* represents the area of the sample (cm^2), *t* represents the time of exposure (h), whereas v_0 and v ($\text{mm}\cdot\text{y}^{-1}$) are the corrosion rates in the absence and presence of corrosion inhibitor, respectively.

$$C_R = \frac{87.6 \cdot W}{d \cdot A \cdot t} \quad (3)$$

$$\%IE = \frac{v_0 - v}{v_0} \cdot 100 \quad (4)$$

2.5. Corrosion Protection Mode Analysis of Oleic-Imidazoline

Analysis of corrosion protection mode of oleic imidazoline was carried out by extracting the corrosion medium solution using CH_2Cl_2 :brine solution (1:1, v/v). The collected organic layer then was identified using TLC with the same condition as previously stated. Further, FTIR characterization was also conducted.

3. Results and Discussion

3.1. Oleic-imidazoline synthesis

In this present study, oleic-imidazoline from TETA and technical grade of OA was successfully synthesized using reflux following the reaction scheme illustrated in Figure 1. According to Figure 1, the formation of oleic-imidazoline consisted of two steps, *i.e.* amidation and cyclization, which involved water elimination in both steps [15]. The using of technical grade of OA will produce oleic-imidazoline in a mixture with other fatty acid-imidazoline, such as linoleic-imidazoline and stearic-imidazoline, but the predominant synthesized compound was oleic-imidazoline, which was confirmed by using FTIR, UV-Vis, NMR (^1H and ^{13}C), and LC-MS/MS spectral data.

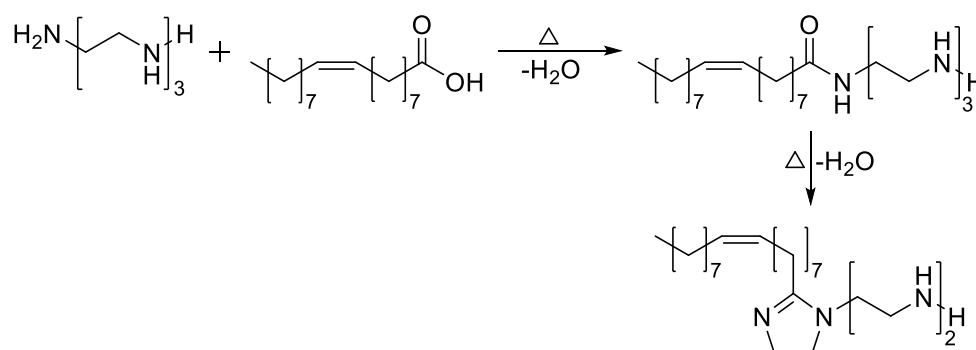


Figure 1. Reaction scheme of oleic-imidazoline synthesis.

FTIR spectra of oleic-imidazoline showed characteristic peaks of imidazoline at wavenumber (ν_{\max}) of 1656.51 and 1271.31 cm^{-1} indicated $\text{C}=\text{N}$ and $=\text{C}-\text{N}$ in imidazoline ring, respectively. In addition, the hydrocarbon chain in the synthesized compound which was formed from unsaturated fatty acid exhibited absorption peaks at ν_{\max} of 3008.25 ($\text{C}-\text{H}$ sp^2), 1643.12 ($\text{C}=\text{C}$), and 723.84 cm^{-1} (*cis* $\text{C}-\text{H}$) together with 2924.75–2853.07 (stretching $\text{C}-\text{H}$ sp^3) and 1465.09–1375.29 cm^{-1} (bending $\text{C}-\text{H}$ sp^3). This compound also showed peaks for stretching $\text{N}-\text{H}$ and bending $\text{N}-\text{H}$ at ν_{\max} of 3291.83 and 1547.80,

respectively, belonging to the pendant group [16]. Moreover, maximum absorbance in UV-Vis spectra of oleic-imidazoline appeared at the wavelength (λ_{\max}) of 203.8 nm, specified as C=N from imidazoline moiety [11–12].

Further characterization then was carried out by using NMR. ^1H NMR (500 MHz, CDCl_3) exhibited characteristic peaks of imidazoline scaffold from unsaturated fatty acid [9, 17]. Peaks at a chemical shift (δ_{H}) of 3.62–3.26 ppm (4H, *m*) indicated the formation of the imidazoline ring, whereas peaks at δ_{H} 2.16 ppm (2H, *t*, 7 Hz) showed the proton on hydrocarbon chain nearest to the imidazoline ring ($\text{H}-\text{C}-\text{C}=\text{N}$). Other protons indicating an unsaturated hydrocarbon chain had appeared at δ_{H} 5.33 (2H, *q*, 7 Hz) for proton attached on C=C alkene, 2.01 (4H, *q*, 7 Hz) for proton adjacent to C=C alkene, and the rest at δ_{H} 1.59 (2H, *qi*, 9.5 Hz), 1.37–1.24 (20H, *m*), 0.87 ppm (3H, *t*, 7 Hz) for the remaining hydrocarbon chain. In addition, peaks from the pendant group pointed at δ_{H} 2.92–2.42 (8H, *m*) correlated to four $-\text{CH}_2$ groups attached to the nitrogen atom which having proton appeared at δ_{H} 4.23 (3H, *br s*). ^{13}C NMR (125 MHz, CDCl_3) showed a specific peak of imidazoline-derived at a chemical shift (δ_{C}) of 164.6 ppm belonging to C=N [18]. Moreover, peaks at δ_{C} 130.1 and 129.9 ppm indicated the C sp^2 from C=C alkene in the unsaturated hydrocarbon chain. Actually, in the C sp^2 region (δ_{C} 130.4–128.0 ppm), there were additional four peaks correlated to two alkenes from linoleic-imidazoline, as another constituent of synthesized oleic-imidazoline from the technical grade of OA. In addition, peaks at δ_{C} 56.7–52.9 ppm corresponded to C sp^3 bonded to the nitrogen atom in both imidazoline ring and pendant group, while peaks at δ_{C} 32.0–14.3 ppm indicated C sp^3 in the hydrocarbon chain.

To analyze the oleic-imidazoline composition, LC-MS/MS spectra were recorded. LC chromatogram of oleic-imidazoline exhibited predominant peak (>80%) at a retention time (rt) of 10.87 min represented oleic-imidazoline with $[\text{M}+\text{H}]^+$ 393.37 m/z, calculated as $\text{C}_{24}\text{H}_{49}\text{N}_4^+$. The proposed selected fragmentation of oleic-imidazoline was illustrated in Figure 2. Two minor peaks were also observed at rt 10.52 and 11.52 min for linoleic- ($[\text{M}+\text{H}]^+$ 391.38 m/z, $\text{C}_{24}\text{H}_{47}\text{N}_4^+$) and stearic-imidazoline ($[\text{M}+\text{H}]^+$ 395.38 m/z, $\text{C}_{24}\text{H}_{51}\text{N}_4^+$), respectively. Oleic-imidazoline exhibited rt between linoleic- and stearic-imidazoline since it was less polar than linoleic-imidazoline but more polar compared to stearic-imidazoline. All the spectrum data indicated that oleic-imidazoline had been successfully synthesized.

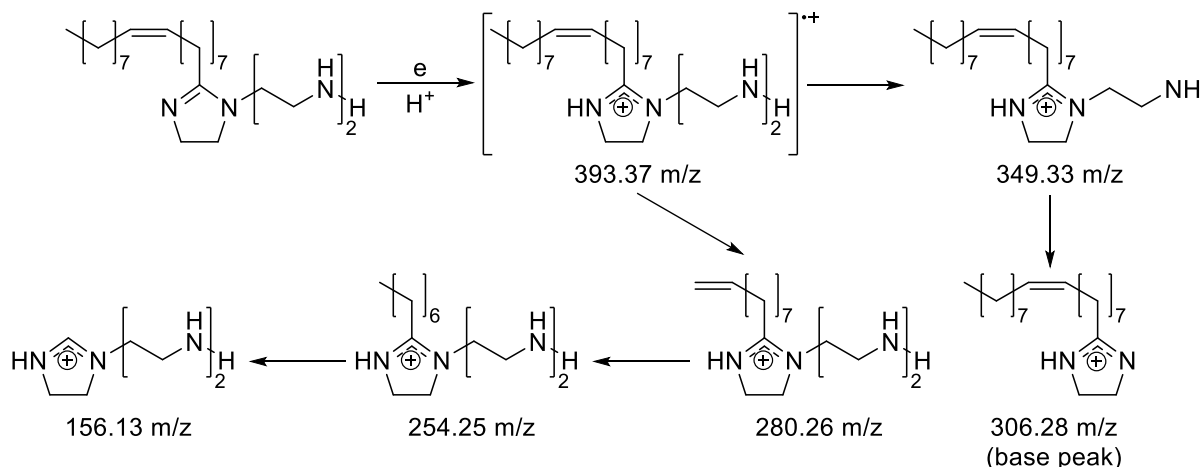


Figure 2. Proposed selected fragmentation scheme of oleic-imidazoline.

3.2. Effect of inhibitor's concentration on Tafel polarization analysis

Tafel polarization curves of the oleic-imidazoline and commercial sample were displayed in Figure 3. Oleic-imidazoline was found to be effective in inhibiting the corrosion of low carbon steel in chloride environments similar to commercial sample. Figure 4 displayed the %*IE* and C_R of both corrosion inhibitors as a function of the inhibitor concentration used on the Tafel polarization method. According to Figure 4, the C_R decreased and therefore the %*IE* improved as the inhibitor concentration was increased. This result exhibited that inhibitor is adsorbed to a larger degree on the metal surface as the inhibitor concentration is increased, which leads to the restriction of interaction between corrosive environment and metal surface [3, 19]. Oleic-imidazoline and commercial sample at 500 ppm demonstrated the best %*IE* as 83.26 and 84.41%, respectively. A slight difference in %*IE* makes the synthesized oleic-imidazoline can be used as an alternative corrosion inhibitor.

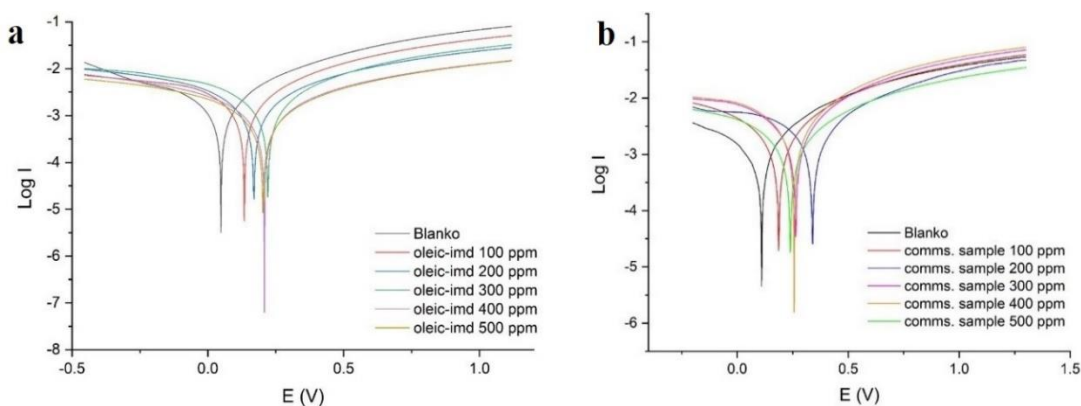


Figure 3. Tafel polarization curves of oleic-imidazoline (a) and commercial sample (b).

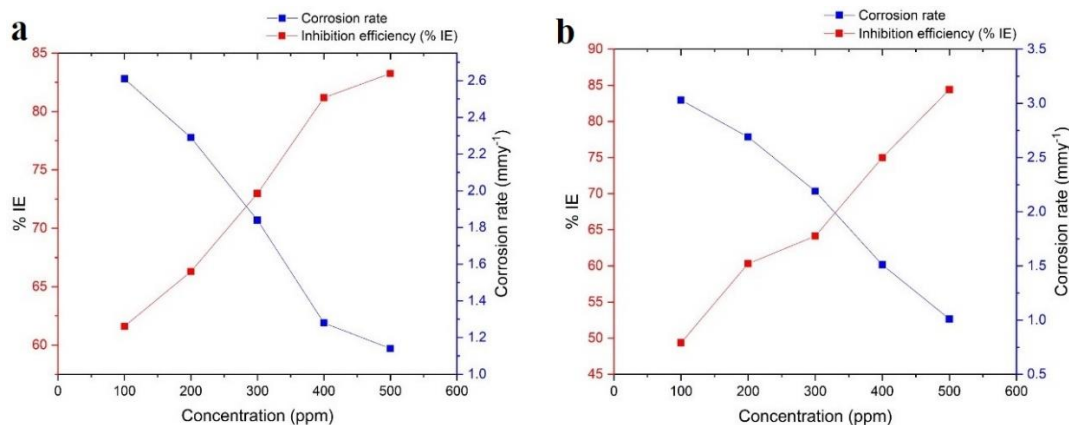


Figure 4. Corrosion rate and percentage of inhibition efficiency with various concentration of oleic-imidazoline (a) and commercial sample (b) using Tafel polarization method.

3.3. Effect of inhibitor's concentration on weight loss analysis

The %IE and C_R of oleic-imidazoline and commercial sample as a function of the inhibitor concentration used on weight loss method was presented in Figure 5. Based on Figure 5, similar trends on %IE and C_R were observed with the previous inhibition corrosion method. With this method, oleic-imidazoline demonstrated a slightly higher %IE at 500 ppm (83.33%) than the commercial sample at the same concentration (500 ppm, 80.00%). The higher %IE of oleic-imidazoline was due to the interaction between electron-donating groups such as imidazoline ring, amino groups in pendant chain, and double-bond (π -electron) in imidazoline ring and hydrocarbon chain [19].

Figure 6 plotted the comparison of the %IE as a function of the inhibitor concentration used for both Tafel polarization and weight loss methods. According to Figure 6, the %IE obtained was not significantly different, especially in a higher concentration of inhibitor. The difference in %IE was probably due to the longer immersion time in the weight loss method which can cause the dissolution of the linkage between metal and inhibitor making the increase of C_R [3]. However, both methods showed that the corrosion of low carbon steel in chloride environments was significantly reduced in the presence of an oleic-imidazoline inhibitor compound.

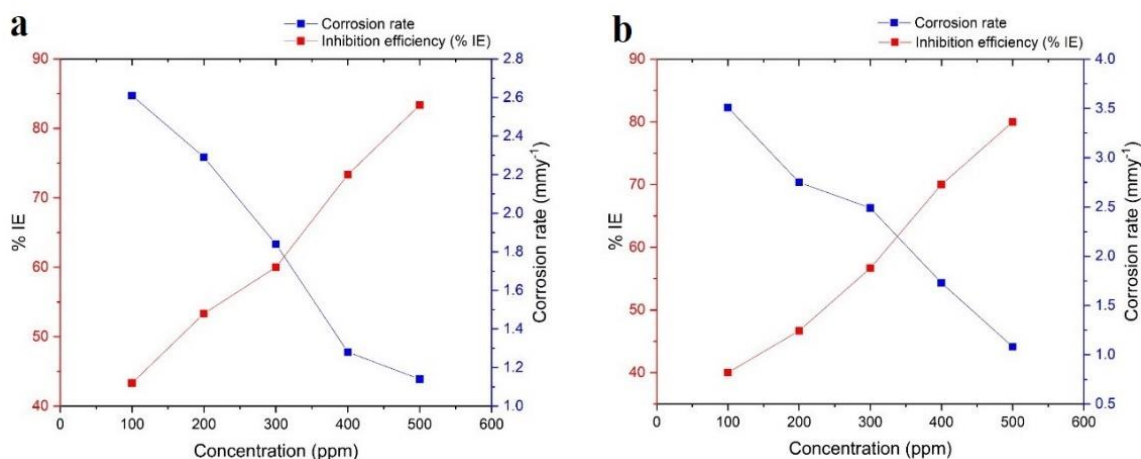


Figure 5. Corrosion rate and percentage of inhibition efficiency with various concentration of oleic-imidazoline (a) and commercial sample (b) using weight loss method.

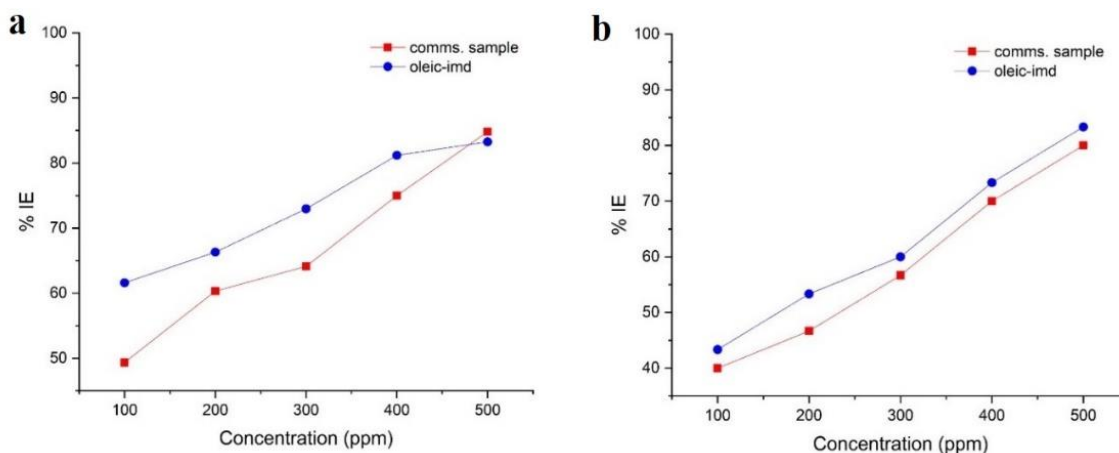


Figure 6. Corrosion inhibition activity of oleic-imidazoline and commercial sample in 1% NaCl using electrochemical (a) and gravimetric (b) methods.

3.4. Corrosion protection mode analysis of oleic-imidazoline

Analysis of corrosion protection mode of oleic-imidazoline was carried out after corrosion inhibition test by using FTIR. The FTIR spectra of oleic-imidazoline before and after corrosion test were presented in Figure 7. By comparing the FTIR spectra in Figure 7, it was observed that there were still typical peaks of imidazoline at ν_{\max} 1654.48 and 1272.39 cm^{-1} belonging to C=N and =C–N in the imidazoline ring, respectively. In addition, it was also detected a new peak in low intensity at ν_{\max} 1725.37 cm^{-1} which indicated the structural change in oleic-imidazoline after the corrosion test. The new peak probably represents C=O amide which indicates the hydrolysis process during the corrosion test (Figure 8). However, since there were still characteristic peaks of imidazoline and only slightly altered the imidazoline ring structure, it can be stated that the corrosion protection mode of oleic-imidazoline was physisorption with slight chemisorption [20].

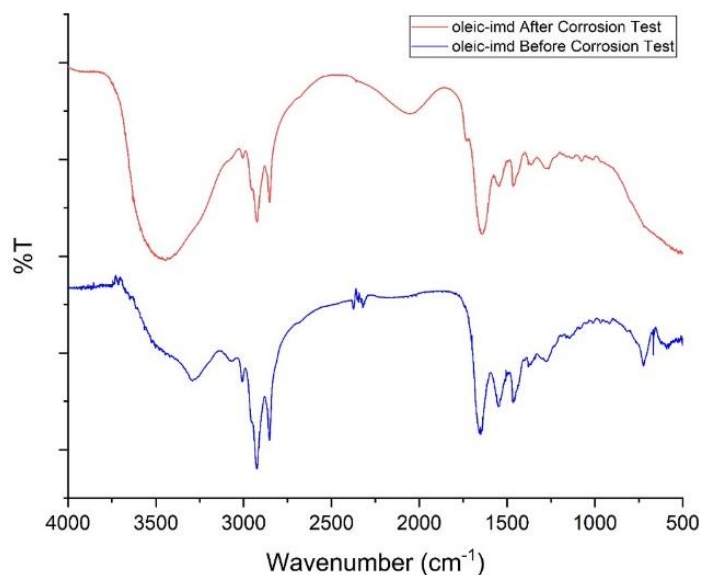


Figure 7. FTIR spectra of oleic-imidazole before and after corrosion test.

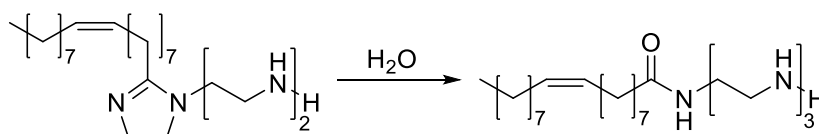


Figure 8. Proposed structural changes of oleic-imidazole after a corrosion test.

The corrosion protection mode of oleic-imidazole was found in agreement with the other organic corrosion inhibitor containing high electron density and long hydrophobic chains [13]. The proposed mechanism of oleic-imidazole's performance on inhibiting corrosion on the metal surface was illustrated in Figure 9. Oleic-imidazole has π -electron and N heteroatoms which are rich in lone pairs, making the adsorption of imidazole on the metal surface. Meanwhile, the hydrocarbon chain forms a hydrophobic layer as a protective film on the metal surface which can block the active site of corrosion on the metal surface from the corrosive environment [21–23]. The adsorption behavior of the protective film is determined by the electrostatic interaction between the heteroatom and the double bond of the corrosion inhibitor and the metal surface [20, 24]. The protective layer of the inhibitor will break the corrosion linkage which allows the π -electron donor of imidazole to the empty orbital of the metal surface resulting in the higher value of %IE [21]. The high %IE value of oleic-imidazole is summarized due to the barrier effect of physical and chemical interactions from the heteroatoms with the metal surface.

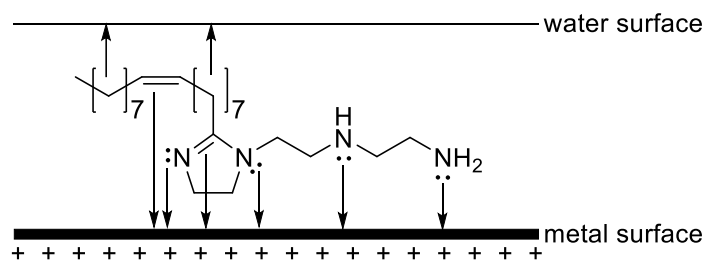


Figure 9. Proposed mechanism of oleic-imidazoline absorption on metal surfaces.

Conclusions

In this research, oleic-imidazoline was successfully synthesized by reacting triethylenetetramine (TETA) and technical grade of oleic acid (OA) under reflux for 12 h at 100–140°C. The structure of the synthesized compound was elucidated by using FTIR, UV-Vis, NMR (^1H and ^{13}C), and LC-MS/MS spectral data. The corrosion inhibitor activity test towards low carbon steel in a 1% NaCl solution indicated that oleic-imidazoline can be used as a potential corrosion inhibitor compared with commercial sample with the highest inhibition efficiency percentage (%IE) was 83.26 and 83.33% in 500 ppm using Tafel polarization and weight loss methods, respectively. The corrosion protection mode of oleic-imidazoline was physisorption with slight chemisorption since the corrosion inhibition test slightly altered the imidazoline ring structure.

Acknowledgement

This work was supported by collaboration between FMIPA Universitas Indonesia and PT. Pertamina (Persero) research grant No. 006/G40200/2020-S0.

References

1. S.S. Al-Shihry, A.R. Sayed and H.M. Abd El-lateef, Design and assessment of a novel poly(urethane-semicarbazides) containing thiadiazoles on the backbone of the polymers as inhibitors for steel pipelines corrosion in CO_2 -saturated oilfield water, *J. Mol. Struct.*, 2020, **1201**, 1–9. doi: [10.1016/j.molstruc.2019.127223](https://doi.org/10.1016/j.molstruc.2019.127223)
2. T. Hong and W.P. Jepson, Corrosion inhibitor studies in large flow loop at high temperature and high pressure, *Corros. Sci.*, 2001, **43**, no. 10, 1839–1849. doi: [10.1016/S0010-938X\(01\)00002-6](https://doi.org/10.1016/S0010-938X(01)00002-6)
3. A. Alamiery, E. Mahmoudi and T. Allami, Corrosion inhibition of low-carbon steel in hydrochloric acid environment using a Schiff base derived from pyrrole: gravimetric and computational studies, *Int. J. Corros. Scale Inhib.*, 2021, **10**, no. 2, 749–765. doi: [10.17675/2305-6894-2021-10-2-17](https://doi.org/10.17675/2305-6894-2021-10-2-17)
4. K.A. Ismaili, S. EL Arouji, A. Abdellaoui, F. El Kamani, Z. Rais, M.F. Baba, M. Taleb, K.M. Emran, A. Zarrouk, A. Aouniti and B. Hammouti, Electrochemical and gravimetric studies of the corrosion inhibition of mild steel in HCl medium by cymbopogon nardus essential oil, *Der Pharma Chem.*, 2001, **7**, no. 10, 34–44.

5. G. Zhang, C. Chen, M. Lu, C. Chai and Y. Wu, Evaluation of inhibition efficiency of an imidazoline derivative in CO₂-containing aqueous solution, *Mater. Chem. Phys.*, 2007, **105**, no. 2–3, 331–340. doi: [10.1016/j.matchemphys.2007.04.076](https://doi.org/10.1016/j.matchemphys.2007.04.076)
6. F.G. Liu, M. Du, J. Zhang and M. Qiu, Electrochemical behavior of Q235 steel in saltwater saturated with carbon dioxide based on new imidazoline derivative inhibitor, *Corros. Sci.*, 2009, **51**, no. 1, 102–109. doi: [10.1016/j.corsci.2008.09.036](https://doi.org/10.1016/j.corsci.2008.09.036)
7. S.A. Umoren, Polypropylene glycol: A novel corrosion inhibitor for × 60 pipeline steel in 15% HCl solution, *J. Mol. Liq.*, 2016, **219**, 946–958. doi: [10.1016/j.molliq.2016.03.077](https://doi.org/10.1016/j.molliq.2016.03.077)
8. G. Bereket and A. Yurt, Inhibition of the corrosion of low carbon steel in acidic solution by selected quaternary ammonium compounds, *Anti-Corros. Methods Mater.*, 2002, **49**, no. 3, 210–220. doi: [10.1108/00035590210431764](https://doi.org/10.1108/00035590210431764)
9. J-M. Zhao, F. Gu, T. Zhao and R-J. Jiang, Corrosion inhibition performance of imidazoline derivatives with different pedant chains under three flow rates in high-pressure CO₂ environment, *Res. Chem. Intermed.*, 2016, **42**, no. 6, 5753–5764. doi: [10.1007/s11164-015-2401-y](https://doi.org/10.1007/s11164-015-2401-y)
10. F. Zhou, H. Wang and Q. Dai, Study on the compound of imidazoline corrosion inhibitor, *IOP Conf. Ser. Earth Environ. Sci.*, 2018, **153**, 1–11. doi: [10.1088/1755-1315/153/5/052001](https://doi.org/10.1088/1755-1315/153/5/052001)
11. M. Mujahiduzzakka, D.U.C. Rahayu, D.A. Nurani and Y.K. Krisnandi, Synthesis of oleic imidazoline derivative using MAOS (microwave assisted organic synthesis) method as corrosion inhibitor towards carbon steel, *AIP Conf. Proc.*, 2020, **2242**, 1–6. doi: [10.1063/5.0008006](https://doi.org/10.1063/5.0008006)
12. M.I. Andra, D.U.C. Rahayu, I. Abdullah and Y.K. Krisnandi, Ester-imidazoline: Modification of imidazoline using MAOS (microwave assisted organic synthesis) method as corrosion inhibitor towards carbon steel, *AIP Conf. Proc.*, 2020, **2242**, no. 1, 1–5. doi: [10.1063/5.0008002](https://doi.org/10.1063/5.0008002)
13. A.G. Berezhnaya, E.S. Khudoleeva and V.V. Chernyavina, Some imidazolines and their mixtures with inorganic anions as inhibitors of acid corrosion of steel, *Int. J. Corros. Scale Inhib.*, 2021, **10**, no. 2, 649–661. doi: [10.17675/2305-6894-2021-10-2-11](https://doi.org/10.17675/2305-6894-2021-10-2-11)
14. D.U.C. Rahayu, D.A. Setyani, H. Dianhar and P. Sugita, Phenolic compounds from Indonesian white turmeric (*Curcuma zedoaria*) rhizomes, *Asian J. Pharm. Clin. Res.*, 2020, **13**, no. 7, 194–198. doi: [10.22159/ajpcr.2020.v13i7.38249](https://doi.org/10.22159/ajpcr.2020.v13i7.38249)
15. V.M. Abbasov, T.A. Mammadova, K.R. Veliyev and K.H. Kasamanli, Hydroxy- and aminoethyl imidazolines of cottonseed oil fatty acids as additives for diesel fuels, *Open J. Synth. Theory Appl.*, 2015, **4**, no. 2, 33–39. doi: [10.4236/ojsta.2015.42004](https://doi.org/10.4236/ojsta.2015.42004)
16. X. Kong, C. Qian, W. Fan and Z. Liang, Experimental and QSAR study on the surface activities of alkyl imidazoline surfactants, *J. Mol. Struct.*, 2018, **1156**, 164–171. doi: [10.1016/j.molstruc.2017.11.102](https://doi.org/10.1016/j.molstruc.2017.11.102)

17. D. Bajpai and V.K. Tyagi, Synthesis and characterization of imidazolium surfactants derived from tallow fatty acids and diethylenetriamine, *Eur. J. Lipid Sci. Technol.*, 2008, **110**, no. 10, 935–940. doi: [10.1002/ejlt.200800046](https://doi.org/10.1002/ejlt.200800046)
18. M.W.S. Jawich, G.A. Oweimreen and S.A. Ali, Heptadecyl-tailed mono- and bis-imidazolines: A study of the newly synthesized compounds on the inhibition of mild steel corrosion in a carbon dioxide-saturated saline medium, *Corros. Sci.*, 2012, **65**, 104–112. doi: [10.1016/j.corsci.2012.08.001](https://doi.org/10.1016/j.corsci.2012.08.001)
19. M.M. Solomon, S.A. Umoren, M.A. Quraishi and M. Salman, Myristic acid based imidazoline derivative as effective corrosion inhibitor for steel in 15% HCl medium, *J. Colloid Interface Sci.*, 2019, **551**, 47–60. doi: [10.1016/j.jcis.2019.05.004](https://doi.org/10.1016/j.jcis.2019.05.004)
20. K. Zhang, W. Yang, B. Xu, Y. Liu, X. Yin and Y. Chen, Corrosion inhibition of mild steel by bromide-substituted imidazoline in hydrochloric acid, *J. Taiwan Inst. Chem. Eng.*, 2015, **57**, 167–174. doi: [10.1016/j.jtice.2015.05.021](https://doi.org/10.1016/j.jtice.2015.05.021)
21. Y. Tang, F. Zhang, S. Hu, Z. Cao, Z. Wu and W. Jing, Novel benzimidazole derivatives as corrosion inhibitors of mild steel in the acidic media. Part I: Gravimetric, electrochemical, SEM and XPS studies, *Corros. Sci.*, 2013, **74**, 271–282. doi: [10.1016/j.corsci.2013.04.053](https://doi.org/10.1016/j.corsci.2013.04.053)
22. A.I. Obike, P.C. Okafor, K.J. Uwakwe, X. Jiang and D. Qu, The inhibition of CO₂ corrosion of L360 mild steel in 3.5% NaCl solution by imidazoline derivatives, *Int. J. Corros. Scale Inhib.*, 2018, **7**, no. 3, 318–330. doi: [10.17675/2305-6894-2018-7-3-3](https://doi.org/10.17675/2305-6894-2018-7-3-3)
23. Ya.G. Avdeev and Yu.I. Kuznetsov, Nitrogen-containing five-membered heterocyclic compounds as corrosion inhibitors for metals in solutions of mineral acids – An overview, *Int. J. Corros. Scale Inhib.*, 2021, **10**, no. 2, 480–540. doi: [10.17675/2305-6894-2020-10-2-2](https://doi.org/10.17675/2305-6894-2020-10-2-2)
24. A.I. Altsybeeveva, E.A. Tronova and V.V. Burlov, Hydrocarbon-soluble metal corrosion inhibitors. II. Physicochemical aspects of inhibitor action. Amides and salts of carboxylic acids, *Int. J. Corros. Scale Inhib.*, 2014, **3**, no. 3, 160–166. doi: [10.17675/2305-6894-2014-3-3-160-166](https://doi.org/10.17675/2305-6894-2014-3-3-160-166)

